DMD Fast Forward. Published on May 15, 2023 as DOI: 10.1124/dmd.123.001326
This article has not been copyedited and formatted. The final version may differ from this version.

Research Article

Drug Metabolism & Disposition

Assumptions Underlying Hepatic Clearance Models: Recognizing the Influence of Saturable Protein Binding on Driving Force Concentration and Discrimination Between Models of Hepatic Clearance

Julia A. Schulz Pauly, Jin Wang, Colin J. Phipps, John Cory Kalvass

Quantitative, Translational & ADME Sciences (QTAS), Abbvie Inc., North Chicago, IL, USA

DMD Fast Forward. Published on May 15, 2023 as DOI: 10.1124/dmd.123.001326
This article has not been copyedited and formatted. The final version may differ from this version.

Running Title: Saturable Plasma Protein Binding in Clearance Predictions

Corresponding Author:

John Cory Kalvass, AbbVie Inc., 1 N. Waukegan Rd, North Chicago, IL, 60064-6118; +1 847-937-8987, j.kalvass@abbvie.com

Number of Pages: 15

Number of Tables: 2

Number of Figures: 3

Number of References: 48

Number of Words in Abstract: 185 words

Number of Words in Introduction: 742 words

Number of Words in Discussion: 1,945 words

Number of Words in Significance Statement: 80 words

List of Nonstandard Abbreviations:

AICc	Simple-size adjusted Akaike's Information Criterion
B_{max}	Maximal binding capacity
C	Concentration
C_{DM}	Concentration driving clearance in dispersion model
C_{in}	Concentration entering the liver
CL_H	Hepatic clearance
$CL_{int,u}$	Unbound intrinsic hepatic clearance
$CL_{int,u,DM}$	Unbound intrinsic hepatic clearance in dispersion model

DMD Fast Forward. Published on May 15, 2023 as DOI: 10.1124/dmd.123.001326
This article has not been copyedited and formatted. The final version may differ from this version.

$CL_{int,u,MWSM}$	Unbound intrinsic hepatic clearance in modified well-stirred model
$CL_{int,u,PTM}$	Unbound intrinsic hepatic clearance in parallel tube model
$CL_{int,u,WSM}$	Unbound intrinsic hepatic clearance in well-stirred model
C_{MWSM}	Concentration driving clearance in modified well-stirred model
C_{out}	Concentration leaving the liver
C_{PTM}	Concentration driving clearance in parallel tube model
C_{WSM}	Concentration driving clearance in well-stirred model
D	Dilution Factor
DM	Dispersion model
D_N	Dispersion number
ER	Extraction ratio
F	Hepatic availability
f_u	Fraction unbound
$f_{u,b}$	Fraction unbound in blood
$f_{u,exp}$	Static equilibrium unbound fraction under protein binding experimental conditions
$f_{u,p}$	Fraction unbound in plasma
$f_{u,sat}$	Saturable fraction unbound
HSA	Human serum albumin
IPRL	Isolated perfused rat liver experiment

DMD Fast Forward. Published on May 15, 2023 as DOI: 10.1124/dmd.123.001326
This article has not been copyedited and formatted. The final version may differ from this version.

IVIVE	*In-vitro-in-vivo* extrapolation
K_D	Equilibrium dissociation constant
K_m	Michaelis-Menten constant
K_{nsb}	Non-saturable binding constant or binding potential
k_{off}	Protein binding off rate
k_{on}	Protein binding on rate
MWSM	Modified well-stirred model
NSB	Non-saturable binding
PTM	Parallel tube model
Q	Perfusion rate
Q_H	Hepatic flow rate
R_{BP}	Blood-to-plasma ratio
R_N	Efficiency number
SB	Saturable binding
SD	Standard deviation
WSM	Well-stirred model

DMD Fast Forward. Published on May 15, 2023 as DOI: 10.1124/dmd.123.001326
This article has not been copyedited and formatted. The final version may differ from this version.

Abstract

One underlying assumption of hepatic clearance models is often underappreciated. Namely, plasma protein binding is assumed to be non-saturable within a given drug concentration range, dependent only on protein concentration and K_D. However, *in vitro* hepatic clearance experiments often use low albumin concentrations that may be prone to saturation effects, especially for high-clearance compounds, where the drug concentration changes rapidly. Diazepam isolated perfused rat liver literature datasets collected at varying concentrations of albumin were used to evaluate the predictive utility of four hepatic clearance models (the well-stirred, parallel tube, dispersion, and modified well-stirred model) while both ignoring and accounting for potential impact of saturable protein binding on hepatic clearance model discrimination. In agreement with previous literature findings, analyses without accounting for saturable binding showed poor clearance prediction using all four hepatic clearance models. Here, we show that accounting for saturable albumin binding improves clearance predictions across the four hepatic clearance models. Additionally, the well-stirred model best reconciles the difference between the predicted and observed clearance data, suggesting that the well-stirred model is an appropriate model to describe diazepam hepatic clearance when considering appropriate binding models.

Keywords: Hepatic Clearance, Saturable Plasma Protein Binding, Albumin, Diazepam, In Vitro-In Vivo Extrapolation

DMD Fast Forward. Published on May 15, 2023 as DOI: 10.1124/dmd.123.001326
This article has not been copyedited and formatted. The final version may differ from this version.

Significance Statement:

Hepatic clearance models are vital for understanding clearance. Caveats in model discrimination and plasma protein binding have sparked an ongoing scientific discussion. This study expands our understanding of the underappreciated potential for saturable plasma protein binding. We recognize that f_u must correspond to relevant driving force concentration. These considerations can improve clearance predictions and address hepatic clearance model disconnects. Importantly, even though hepatic clearance models are simple approximations of complex physiological processes, they are valuable tools for clinical clearance predictions.

DMD Fast Forward. Published on May 15, 2023 as DOI: 10.1124/dmd.123.001326
This article has not been copyedited and formatted. The final version may differ from this version.

Introduction

"All models are wrong, some are useful." – (Box, 1976)

This paradigm can be applied to all model systems used in drug development. But one area where it becomes abundantly clear is hepatic clearance models. These models are vital for enabling *in-vitro-in-vivo* extrapolation (IVIVE) of hepatic clearance and predicting drug-drug interactions and population differences (e.g., genetic polymorphisms). However, physiological relevance and prediction accuracy vary (Ito and Houston, 2005; Camenisch and Umehara, 2012; Poulin *et al.*, 2012).

Three hepatic clearance models are commonly employed: the well-stirred model (WSM; **Eq.1**), parallel tube model (PTM; **Eq.2**), and dispersion model (DM; **Eq.3**). These three models describe different relationships between hepatic clearance (CL_H), hepatic flow rate (Q_H), unbound fraction in the experimental system (f_u) and unbound intrinsic hepatic clearance ($CL_{int,u}$). $CL_{int,u}$ is the ability of the liver to clear a compound, independent of Q_H and f_u (Jones *et al.*, 1984; Benet *et al.*, 2018; Benet and Sodhi, 2020; Rowland *et al.*, 2021).

$$WSM: CL_H = \frac{Q_H \times f_u \times CL_{int,u,WSM}}{Q_H + f_u \times CL_{int,u,WSM}} \quad (1)$$

$$PTM: CL_H = Q_H \left(1 - e^{-f_u \times CL_{int,u,PTM} / Q_H}\right) \quad (2)$$

$$DM: CL_H = Q_H \left(1 - \frac{4a}{(1+a)^2 \times e^{-(1-a)/2D_N} - (1-a)^2 \times e^{-(1+a)/2D_N}}\right) \quad (3)$$

$$a = \sqrt{1 + 4D_N \frac{f_u \times CL_{int,u,DM}}{Q_H}} \quad (3a)$$

In vivo, the f_u can be either the f_u in blood ($f_{u,b}$) or plasma ($f_{u,p}$), which should be corrected for the blood-to-plasma ratio (R_{BP}). However, in *in vitro* and *ex vivo* systems, the f_u represents the experimentally measured f_u ($f_{u,exp}$) in the respective system. Additionally, Q_H can refer to the *in vivo* hepatic blood flow or an experimental perfusion rate.

DMD Fast Forward. Published on May 15, 2023 as DOI: 10.1124/dmd.123.001326
This article has not been copyedited and formatted. The final version may differ from this version.

The main differences between the three hepatic models are the applied flow and extent of mixing. The WSM assumes that the system is instantaneously well mixed (Pang and Rowland, 1977a; Rowland *et al.*, 2021). In contrast, the PTM assumes that the liver consists of identical parallel tubes with evenly distributed enzymes without mixing (Pang and Rowland, 1977a; Rowland *et al.*, 2021). Finally, the DM is an intermediate state between WSM and PTM with different degrees of mixing described by the dispersion number (D_N), estimated with non-eliminated markers (Roberts and Rowland, 1986b). The WSM and PTM are extreme cases of the DM where D_N is infinity or zero, respectively (Roberts and Rowland, 1986a; Diaz-Garcia *et al.*, 1992).

Recently, an additional fourth model of hepatic clearance was introduced, the modified well-stirred model (MWSM; **Eq.4**; (Hsu *et al.*, 2021)).

$$MWSM: CL_H = f_u \times CL_{int,u,MWSM} \quad (4)$$

However, the MWSM does not follow the common assumption that $CL_{int,u,MWSM}$ is independent of Q_H (Hsu *et al.*, 2021).

While there are theoretical differences, the hepatic clearance models are built on shared fundamental assumptions. First, the models are derived from Michaelis-Menten kinetics, Fick's diffusion principle, and mass balance considerations (Pang and Rowland, 1977a; Michaelis *et al.*, 2011). Second, the definition of CL_H is model-independent and only dependent on Q_H and the extraction ratio (ER; **Eq.5**; (Rowland and Pang, 2018, 2022; Korzekwa and Nagar, 2023)). ER, a measure of elimination efficiency, can be determined from the concentration entering (C_{in}) and leaving the liver (C_{out}).

$$CL_H = Q_H \times ER = Q_H \times (1 - F) = Q_H \times \frac{C_{in} - C_{out}}{C_{in}} \quad (5)$$

Third, drugs establish a rapid equilibrium between sinusoidal, extracellular and intracellular spaces (Pang and Rowland, 1977a; Roberts and Rowland, 1986a). Fourth, drugs are fully bioavailable, e.g., after intravenous dosing. Fifth, clearance occurs only in the liver, thus total

DMD Fast Forward. Published on May 15, 2023 as DOI: 10.1124/dmd.123.001326
This article has not been copyedited and formatted. The final version may differ from this version.

body clearance should be corrected for other organ clearances, including renal clearance (Jusko and Li, 2021; Rowland *et al.*, 2021; Rowland and Pang, 2022).

And finally, hepatic clearance is based on the free drug hypothesis. Therefore, only unbound drug is available for elimination (Pang and Rowland, 1977a; Roberts and Rowland, 1986a). Furthermore, plasma protein binding is typically considered linear or non-saturable, characterized by fast on- (k_{on}) and off-rates (k_{off}), and f_u is assumed to be constant throughout the entire liver (Roberts and Rowland, 1986a; Bteich, 2019).

When comparing the influence of changes in f_u across clearance models, $CL_{int,u}$ predictions are consistent for low ER drugs (Pang and Rowland, 1977a). However, predictions for high ER compounds can vary significantly depending on the applied model (Pang and Rowland, 1977b; Rowland *et al.*, 1984; Hale *et al.*, 1991; Sodhi *et al.*, 2020).

Common explanations for poor clearance predictions and discrepancies among models are lack of physiological relevance, use of incorrect reference concentrations, and theoretical issues with the applied hepatic clearance models (Rowland *et al.*, 1973; Pang and Rowland, 1977b; Roberts and Rowland, 1986a; Diaz-Garcia *et al.*, 1992; Benet and Sodhi, 2020, 2022; Kochak, 2020; Sodhi *et al.*, 2020). However, several underlying assumptions have not been thoroughly tested and could explain the discrepancies.

While further evaluation of the principles of Michaelis-Menten kinetics and non-rate-limiting plasma protein binding may be beneficial, it appears that these assumptions are met in traditional IVIVE approaches (Pang and Rowland, 1977b; Yasumori *et al.*, 1993; Baker and Parton, 2007; Michaelis *et al.*, 2011). Therefore, we focus on the assumption that plasma protein binding is linear, not saturable. If f_u is saturable, it may change throughout the liver and differ between C_{in} and C_{out}. Therefore, we hypothesize that the lack of prediction accuracy may be caused by poor understanding of the dynamic binding processes and application of incorrect, linear f_u terms.

DMD Fast Forward. Published on May 15, 2023 as DOI: 10.1124/dmd.123.001326
This article has not been copyedited and formatted. The final version may differ from this version.

To test the effect of saturable plasma protein binding on hepatic clearance model discrimination, we explored a high-quality IPRL dataset comparing diazepam clearance at different human serum albumin (HSA) concentrations (Wang and Benet, 2019; Hsu *et al.*, 2021). While there is data available on many experimental models and drugs, we chose diazepam for our case study as this IPRL dataset provided the richest data source for albumin-related changes in CL_H. This case study serves as a universal reminder to test and carefully consider all underlying assumptions when applying CL_H models.

DMD Fast Forward. Published on May 15, 2023 as DOI: 10.1124/dmd.123.001326
This article has not been copyedited and formatted. The final version may differ from this version.

Methods

IPRL and equilibrium dialysis data, initially published by Wang and Benet at the University of California San Francisco, USA (Wang and Benet, 2019), and Hsu et al. at the National Defense Medical Center, Taipei, Taiwan (Hsu *et al.*, 2021), were analyzed to evaluate the impact of saturable plasma protein binding on hepatic clearance model discrimination. The original data and key experimental parameters are summarized in **TableS1**.

Saturable Plasma Protein Binding: The dilution factor (D) was calculated by comparing the HSA concentration in plasma (4%) to that in the perfusate (**Eq.6**).

$$D = \frac{\%HSA\ in\ Whole\ Plasma}{\%HSA\ in\ Perfusate} \quad (6)$$

Saturable and non-saturable binding parameters were estimated based on **Eq.7** (Kalvass *et al.*, 2018). The saturable unbound fraction ($f_{u,sat}$) is determined by the maximal binding capacity (B_{max}), protein binding dissociation constant (K_D), and non-saturable binding constant or binding potential (K_{nsb}). These parameters were estimated from the plasma protein binding data (Wang and Benet, 2019; Hsu *et al.*, 2021) with **Eq.7** using GraphPad Prism 9.1.0 with $1/X^2$ weighting (GraphPad Software, San Diego, CA, USA).

$$f_{u,sat} = \frac{C-\left(\frac{Bmax}{D}+K_D\left(1+\frac{K_{nsb}}{D}\right)\right)+\sqrt{\left(C-\left(\frac{Bmax}{D}+K_D\left(1+\frac{K_{nsb}}{D}\right)\right)\right)^2+4K_D\left(1+\frac{K_{nsb}}{D}\right)C}}{2\left(1+\frac{K_{nsb}}{D}\right)C} \quad (7)$$

$$K_{nsb} = \frac{B_{max,nsb}}{K_{D,nsb}} \quad (7a)$$

where C is the total diazepam concentration used for equilibrium dialysis; C=1 μg/ml=3.512 μM in both experiments (Wang and Benet, 2019; Hsu *et al.*, 2021).

Eq.7 includes two binding components, saturable (SB) and non-saturable (NSB), that were considered separately and together, creating three distinct protein binding models. First, plasma protein binding follows the full model, including saturable and non-saturable binding components (SB + NSB). Second, albumin binding is non-saturable (NSB only); therefore, B_{max}

DMD Fast Forward. Published on May 15, 2023 as DOI: 10.1124/dmd.123.001326
This article has not been copyedited and formatted. The final version may differ from this version.

is 0 (Bteich, 2019). The third model considers only saturable plasma protein binding while constraining K_{nsb} to 0 (SB only). Model fits were compared using the weighted R^2 and the sample-size adjusted Akaike's Information Criterion (AICc) determined in GraphPad Prism 9.1.0.

Concentration-dependent changes in diazepam $f_{u,sat}$ were modeled at different HSA concentrations and dilution factors D using the estimated parameters and **Eq.7**.

Hepatic Clearance: Overall hepatic clearance (CL_H), extraction ratio (ER), and hepatic availability (F) were calculated for each HSA concentration with the model-independent **Eq.5** (Rowland *et al.*, 1973; Rowland and Pang, 2018; Wang and Benet, 2019).

Hepatic clearance is driven by different concentrations depending on mixing and dispersion factors applied in the respective models. According to the WSM, the concentration is the same across the entire organ and equal to the concentration C_{out}, which drives clearance (**Eq.8**; (Pang and Rowland, 1977a; Rowland *et al.*, 2021)). In the PTM, the drug concentration continuously decreases throughout the liver until it reaches C_{out} at the portal vein. Under these conditions, hepatic clearance is driven by the logarithmic average of C_{in} and C_{out} (**Eq.9**; (Pang and Rowland, 1977a; Rowland *et al.*, 2021)). The driving concentration in the DM is the average hepatic concentration with is determined by the extent of drug distribution in the hepatic blood compartment and the D_N (**Eq.10**; (Roberts and Rowland, 1986a; Diaz-Garcia *et al.*, 1992; Rowland *et al.*, 2021)). On the other hand, the MWSM assumes that hepatic clearance is driven by C_{in} rather than the hepatic concentration (**Eq.11**; (Wang and Benet, 2019; Hsu *et al.*, 2021)).

The driving concentrations, C_{WSM}, C_{PTM}, C_{DM}, and C_{MWSM}, were determined using **Eq.8-11** (Benet *et al.*, 2021; Hsu *et al.*, 2021). In the following step, the respective $f_{u,sat}$ were calculated using **Eq.7** and the estimated binding parameters, C_{in}, and C_{out}.

$$C_{WSM} = C_{out} \quad (8)$$

$$C_{PTM} = \frac{C_{in} - C_{out}}{ln\, C_{in} - ln\, C_{out}} \quad (9)$$

DMD Fast Forward. Published on May 15, 2023 as DOI: 10.1124/dmd.123.001326
This article has not been copyedited and formatted. The final version may differ from this version.

$$C_{DM} = Q_H \times \frac{C_{in} - C_{out}}{CL_H} \approx C_{in} \quad (10)$$

$$C_{MWSM} = C_{in} \quad (11)$$

The relationship between hepatic availability (F) and the HSA concentration in each hepatic clearance model (**Eq.12-15**) was fitted to the experimental data in GraphPad Prism 9.1.0 using 1/Y weighting.

$$F_{WSM} = 1 - \frac{f_u \times CL_{int,u,WSM}}{Q_H + f_u \times CL_{int,u,WSM}} \quad (12)$$

$$F_{PTM} = e^{-f_u \times CL_{int,u,PTM} / Q_H} \quad (13)$$

$$F_{DM} = e^{1-\alpha / 2D_N} = e^{1-\sqrt{1+4D_N R_N} / 2D_N} \quad (14)$$

$$F_{MWSM} = 1 - \frac{f_u \times CL_{int,u,MWSM}}{Q_H} \quad (15)$$

D_N for these experiments was previously reported (D_N=0.34 (Diaz-Garcia ***et al.***, 1992)).

The respective $CL_{int,u}$ values were fitted and used to model ER and CL_H. Model fit was evaluated using the weighted R^2 and AICc provided by GraphPad Prism 9.1.0.

DMD Fast Forward. Published on May 15, 2023 as DOI: 10.1124/dmd.123.001326
This article has not been copyedited and formatted. The final version may differ from this version.

Results

Saturable Albumin Binding

Diazepam binding to HSA was best described by a single-site saturable binding model (B_{max}=136.8 μM, K_D=0.914 μM, K_{nsb}=0 μM; R^2=0.9882; AICc=-193.7; **Fig.1A**; **Table1**).

Additionally, the diazepam concentration-dependent change in $f_{u,sat}$ at different HSA concentrations was evaluated (**Fig.1B**; **Fig.S1**). At the diazepam concentration used in the IPRL experiments (3.512 μM, open circles), protein binding saturation is more pronounced at low (0.025-0.1%; **Fig.S1B**) than at high HSA concentrations (1-4%; **Fig.S1C**).

Hepatic Clearance Predictions

The WSM (solid green line; **Fig.2A**; **Table2**) best described the observed diazepam F, followed by the DM (dashed purple line) and PTM (dashed red line). Introducing the MWSM did not significantly improve the data fitting when saturable albumin binding was considered (blue dotted line; **Fig.2A**; **Table2**). The same model rank order was observed for other clearance measures, such as ER and CL_H (**Fig.2B**; **Fig.S2A-C**).

Additionally, $f_{u,sat}$ for the respective model-dependent driving concentrations (**Fig.S2**; **Table2**) better described the observed diazepam clearance data for each of the four hepatic clearance models than the measured $f_{u,exp}$ at C_{in} (3.512 μM), across all three clearance parameters (F, ER, and CL_H).

$CL_{int,u}$ is independent of $f_{u,exp}$ and, therefore, should not vary with the HSA concentration; the observed $CL_{int,u}$ should be similar to the model fitted $CL_{int,u}$ (**Fig.3; Table2**). The average fold deviation (AFD) was calculated as the ratio of the observed to the fitted $CL_{int,u}$. The AFD was close to 1 for the WSM (**Fig.3**; **Table2**; green circle) and using $f_{u,sat}$ (solid green circle; AFD=1.2) decreased the variability in the data compared to $f_{u,exp}$ (open green circle; AFD=1.6). The AFD deviated from unity by more than 3-fold for the DM (**Fig.3**; **Table2**; purple diamond), PTM (red square), and MWSM (blue triangle), independent of saturable (closed symbols; AFDs for PTM: 3.8, DM: 3.1, MWSM: 3.1) or linear binding (open symbols; AFDs for PTM: 3.7, DM: 3.3,

DMD Fast Forward. Published on May 15, 2023 as DOI: 10.1124/dmd.123.001326
This article has not been copyedited and formatted. The final version may differ from this version.

MWSM: 3.3). The DM and MWSM deviate most at low HSA concentrations, while the PTM deviates more at high HSA concentrations for both $f_{u,exp}$ and $f_{u,sat}$ (**Fig.3**).

DMD Fast Forward. Published on May 15, 2023 as DOI: 10.1124/dmd.123.001326
This article has not been copyedited and formatted. The final version may differ from this version.

Discussion

As outlined in the introduction, we hypothesize that the lack of clearance prediction accuracy may be caused by poor understanding of the dynamic binding processes and application of incorrect f_u terms. The static equilibrium $f_{u,exp}$ may not accurately reflect the dynamic binding processes *in vitro* and *in vivo*.

Here, we show that albumin binding of diazepam is saturable at low HSA concentrations. Therefore, $f_{u,sat}$ changes with the drug concentration or plasma protein dilution factor. Saturable albumin binding parameters were determined from the protein binding data (**Fig.1**; **Fig.S1**; **Table1**) and used to model hepatic clearance. Saturable diazepam binding better described the observed F and CL_H measurements and predicted $CL_{int,u}$ across all four hepatic clearance models (**Fig.2**; **Fig.3**; **Fig.S2&3**; **Table2**; **TableS2**). Overall, the WSM fits the observed clearance data the best across all HSA concentrations and clearance endpoints (**Fig.2**; **Fig.3**; **Fig.S2**).

Saturable plasma protein binding has been well described for α-1-acid glycoprotein (Smith and Waters, 2018; Bteich, 2019). On the other hand, only a few examples of saturation of albumin binding in plasma have been reported. Cefazolin $f_{u,p}$ increases with drug concentration *in vitro* in spiked human plasma and *ex vivo* patient plasma samples and varied within the same patient at trough and peak concentrations (Vella-Brincat *et al.*, 2007). Other examples of saturable albumin binding include valproic acid, indomethacin, ceftriaxone, and temocillin (Bowdle *et al.*, 1980; Alexandre and Fantin, 2018; Nation *et al.*, 2018). Based on our predictions, saturation of plasma protein binding is unlikely at clinically relevant diazepam concentrations (C_{max} = 0.28-2.21 μM (Cortellis, 2022)) in human plasma (4% HSA; **Fig.1B; Fig.S1C**). However, *in vitro* assays are often run at lower plasma protein levels. Therefore, *in vitro* clearance measurements may be more prone to saturation of plasma protein binding (**Fig.S1B**), which may contribute to IVIVE disconnects. Based on these observations, we recommend performing *in vitro* assays at physiologically relevant plasma protein and drug concentrations (4% HSA, 100% plasma), as

DMD Fast Forward. Published on May 15, 2023 as DOI: 10.1124/dmd.123.001326
This article has not been copyedited and formatted. The final version may differ from this version.

recently outlined for experimental best practices (Schulz *et al.*, 2023). Alternatively, plasma protein binding parameters can be fitted using **Eq.7** and applied to the relevant assay conditions.

Additional experimental caveats should be considered. The determined B_{max} (136 µM; **Table1**) is lower than the albumin plasma concentration (~700 µM) and the potential binding site concentration (n=1, ~700 µM (Watkins *et al.*, 1994; Krause and Goss, 2018)). This discrepancy may be explained by considering that albumin binding sites can be occupied by other endogenous ligands, such as bilirubin or fatty acids (Koch-Weser and Sellers, 1976; Inoue *et al.*, 1985; Weisiger, 1985; Zucker *et al.*, 1995). Significant differences in binding are reported for native and fatty acid-free albumin (Rowland *et al.*, 1984; Fujino *et al.*, 2018; Li *et al.*, 2020). This competition prevents drug binding, and saturation may occur at lower drug concentrations.

Several groups have explored diazepam IPRL at varying HSA concentrations for hepatic clearance model discrimination (Rowland *et al.*, 1984; Diaz-Garcia *et al.*, 1992; Wang and Benet, 2019; Hsu *et al.*, 2021). The impact of different binding processes on diazepam clearance, including non-specific binding to tubing and other perfusion equipment, was evaluated. While non-specific binding was not observed in the original studies (Rowland *et al.*, 1984; Diaz-Garcia *et al.*, 1992), Wang and Benet reported that $f_{u,exp}$ did not reach 100%, even in HSA-free buffer, indicating drug loss due to non-specific binding (Wang and Benet, 2019). Additionally, $f_{u,exp}$ does not depend on the diazepam concentration if albumin is in excess of the drug and most binding sites are available (Rowland *et al.*, 1984). However, this may not be the case with low HSA concentrations. Furthermore, the authors discussed that $f_{u,exp}$ may change during the liver passage. Yet, the $f_{u,exp}$ measured with equilibrium dialysis was not significantly different in perfusate and effluent. Therefore, $f_{u,exp}$ was assumed to be constant for each HSA concentration (Rowland *et al.*, 1984).

DMD Fast Forward. Published on May 15, 2023 as DOI: 10.1124/dmd.123.001326
This article has not been copyedited and formatted. The final version may differ from this version.

However, the lowest albumin concentration in Rowland's study (1%) does not show saturation based on our modeling results (**FigureS1**; (Rowland *et al.*, 1984)) and the changes in $f_{u,exp}$ may not be apparent under these conditions.

In previous diazepam IPRL studies, a significant change in diazepam F was observed when the protein concentration was low ($f_{u,exp}$~1), while clearance was attenuated in the presence of albumin (Rowland *et al.*, 1984; Diaz-Garcia *et al.*, 1992; Wang and Benet, 2019; Hsu *et al.*, 2021). Additionally, model discrimination is only possible at low HSA concentrations when diazepam is rapidly cleared (Diaz-Garcia *et al.*, 1992; Wang and Benet, 2019; Hsu *et al.*, 2021).

As previously shown, clearance of diazepam in IPRL was better described by the WSM or PTM than DM (Rowland *et al.*, 1984; Diaz-Garcia *et al.*, 1992; Wang and Benet, 2019). However, Hsu et al. claimed that the WSM is only superior at high HSA concentrations ($f_{u,exp}$<0.8). At low HSA concentrations ($f_{u,exp}$>0.8), the MWSM better predicts diazepam availability (Hsu *et al.*, 2021). The authors propose the MWSM as an extreme case where drugs are highly unbound, and C_{in} drives clearance. However, we were unable to confirm this finding.

In our hands, the MWSM performed poorly, both with $f_{u,exp}$, and when considering saturable protein binding, while the WSM most accurately predicted diazepam F in both cases (**Fig.2**; **Fig.3**; **Fig.S2**; **Table2**). However, we should note that our analysis is based on the HSA concentration, while previous evaluations have compared changes in F with f_u (Rowland *et al.*, 1984; Diaz-Garcia *et al.*, 1992; Wang and Benet, 2019; Hsu *et al.*, 2021). This change was necessary since $f_{u,sat}$ is different for each model. Therefore, data comparison across hepatic clearance models was only possible when plotting F against HSA concentration. To compare our data with the previously published results, we included the comparison using f_u in the supplemental information (**Fig.S3**).

For the data analysis, several experimental considerations should be examined. First, in the presence of HSA, C_{DM} is approximately the same as C_{in} throughout the perfusion. Therefore,

DMD Fast Forward. Published on May 15, 2023 as DOI: 10.1124/dmd.123.001326
This article has not been copyedited and formatted. The final version may differ from this version.

there is no significant difference between the $f_{u,sat}$ for the DM and MWSM. However, the model fit varies significantly.

Second, each perfusion started and ended with the 0% HSA group to ensure that the clearance capacity of the liver did not change throughout the experiment (Wang and Benet, 2019; Sodhi *et al.*, 2020; Hsu *et al.*, 2021). While ER is similar for the repetitions, F, C_{out}, and $CL_{int,u}$ vary drastically. The discrepancy between the two endpoints is likely due to non-specific binding to the apparatus and tissue, which is more pronounced during the first perfusion cycle and likely saturated at later time points. Therefore, we only included the 0% HSA data from the end of the perfusions in our analysis. However, since the 0% HSA data points may be problematic due to non-specific binding and potential loss of enzyme activity, we also analyzed all HSA concentrations (0.025-2%), excluding 0% (**Fig.S4**; **TableS2**). While the $CL_{int,u}$ estimates for each model changed slightly, the overall model discrimination and rank order remained the same. Therefore, inclusion or exclusion of the 0% HSA condition did not affect data interpretation.

Third, the D_N used in this study and the original publications was a literature value (D_N=0.34) and not measured in the respective liver preparations (Diaz-Garcia *et al.*, 1992; Wang and Benet, 2019; Hsu *et al.*, 2021). The D_N is generally determined with non-cleared reference markers, such as red blood cells or sucrose. Including these controls in each IPRL experiment could improve the model fit of the DM by correcting for the dispersion processes in the respective liver preparations. The importance of accurate D_N determination is further highlighted by a recent analysis by Sodhi et al. which found that D_N fitted from IPRL experiments with cleared compounds are often large, causing the DM to approach the WSM (Sodhi *et al.*, 2020).

Additionally, several theoretical phenomena must be carefully considered for hepatic model discrimination. First, since clearance is model-independent, all hepatic clearance models have the same value for F, ER, and CL_H (Jusko and Li, 2021; Rowland *et al.*, 2021; Rowland and Pang, 2022; Korzekwa and Nagar, 2023). However, depending on the degree of mixing and flow patterns, the $CL_{int,u}$ values vary significantly (Yadav *et al.*, 2021).

DMD Fast Forward. Published on May 15, 2023 as DOI: 10.1124/dmd.123.001326
This article has not been copyedited and formatted. The final version may differ from this version.

Second, any clearance measure can be helpful for a first critical model examination (Pang and Rowland, 1977a; Jones *et al.*, 1984). However, based on previous experiments, ER appears to be a poor model discriminator because it differs least when CL_H is high, which is "easy" to predict, and is most sensitive to Q_H (Pang and Rowland, 1977b). Therefore, F appeared to be the most appropriate model discriminator and was used in this study (Rowland *et al.*, 1984). Furthermore, the original analysis of these IPRL data focused on F as a clearance parameter (Wang and Benet, 2019; Hsu *et al.*, 2021) and using the same parameter in our analysis allows direct comparison with the original data interpretation.

Third, hepatic clearance models have distinct physiological relevance. The WSM is considered the least physiological model of hepatic clearance since it assumes instantaneous well-stirred conditions. However, when looking at branching, anastomosis, and mixing within the interconnected system of the liver sinusoid, the WSM may accurately describe physiological processes (Pang and Rowland, 1977b). Similar assumptions also underlie the DM, where local movements against flow direction improve mixing, especially at branch points (Roberts and Rowland, 1986a). On the other hand, the MWSM does not follow the definition of $CL_{int,u}$, which is independent of protein binding and Q_H (Jones *et al.*, 1984; Benet *et al.*, 2018; Benet and Sodhi, 2020; Rowland *et al.*, 2021). While the MWSM includes f_u, it does not correct for Q_H (Benet *et al.*, 2018; Hsu *et al.*, 2021). Therefore, it is biased to highly bound, low ER predictions where the hepatic clearance models cannot be distinguished. The MWSM has no physiological relevance for high ER compounds, such as diazepam, where Q_H limits clearance. Therefore, the utility of the MWSM may be limited.

Fourth, it is important to distinguish between blood and plasma CL_H when performing IVIVE, especially when the explored drugs partition into blood cells or bind to blood components other than plasma proteins (Yang *et al.*, 2007; Rowland *et al.*, 2021). However, since IPRLs were performed with Krebs-Ringer bicarbonate buffer containing only diazepam and HSA, with no cells or other blood components, we can assume that the blood to plasma ratio is 1 and

DMD Fast Forward. Published on May 15, 2023 as DOI: 10.1124/dmd.123.001326
This article has not been copyedited and formatted. The final version may differ from this version.

distinction between $f_{u,b}$ and $f_{u,p}$ is not necessary. Therefore, the relevant measured $f_{u,exp}$ and modeled $f_{u,sat}$ values were used for the modeling exercises.

Lastly, while the diazepam saturable binding data presented here provides a promising strategy for improving CL_H predictions, additional compounds and assay formats should be explored to evaluate the potential impact of saturable plasma protein binding. Other IPRL datasets were explored for assessment of saturable binding, but did not provide sufficient information for conclusive analysis, due to the lack of data at very low HSA concentrations (Pang and Rowland, 1977b; Jones *et al.*, 1984; Roberts and Rowland, 1986b). Nevertheless, this analysis provides an important first step to understanding underlying misconceptions and disconnects concerning plasma protein binding in CL_H predictions.

As an aside, saturable plasma protein binding may partially explain observed plasma protein-mediated uptake effects (PMUE). As outlined in our recent review paper on the topic (Schulz *et al.*, 2023), we believe that other alternative explanations, such as saturable plasma protein binding, can consolidate the observed PMUE under the free drug hypothesis (Schulz *et al.*, 2023). If plasma protein binding is saturated, the $f_{u,sat}$ available for clearance is larger than expected based on linear binding assumptions. Therefore, $CL_{int,u}$ appears larger, which has been attributed to PMUE (Schulz *et al.*, 2023). In the present analysis, $CL_{int,u}$ increases with increasing HSA, when considering linear $f_{u,exp}$, which could be interpreted as PMUE. However, $CL_{int,u}$ is constant across the HSA concentrations when correcting for saturable plasma protein binding in the WSM. Therefore, PMUE may be an artifact of applying inaccurate f_u values and violating underlying model assumptions. However, further exploring the contribution of saturable binding to PMUE goes beyond the scope of this manuscript.

Finally, in concordance with George Box (Box, 1976), we demonstrate that “all models are wrong, but some are useful.” Careful testing of all underlying assumptions is vital for proper model application. To this end, we evaluated the linear binding assumption underlying hepatic clearance models.

DMD Fast Forward. Published on May 15, 2023 as DOI: 10.1124/dmd.123.001326
This article has not been copyedited and formatted. The final version may differ from this version.

The intent of this work was to evaluate the assumptions underlying hepatic clearance models applicable to *in vitro*, *ex vivo* and *in vivo* models. Rather than predicting a distinct physiologically relevant *in vivo* CL_H, we evaluated the predicted CL_H as a function of changing experimental conditions. To this end, consideration of saturable plasma protein binding improved hepatic clearance predictions for diazepam. High-clearance compounds, where the concentration changes rapidly and significantly throughout the experiment, may be prone to this phenomenon. Most importantly, saturable binding can reconcile the observed clearance data under the WSM, which described the observed clearance processes well, showing that while clearance models may not be physiologically sound, they can be useful for clearance predictions. Introducing new hepatic clearance models does not improve clearance predictions when $f_{u,sat}$ values are employed. Further research should focus on enhancing f_u measurements and predictions, as a better understanding of binding processes will improve our understanding of the mechanisms underlying IVIVE disconnects. In addition to saturable protein binding, other potential causes of poor f_u predictions should be evaluated, including rate-limiting dissociation.

DMD Fast Forward. Published on May 15, 2023 as DOI: 10.1124/dmd.123.001326
This article has not been copyedited and formatted. The final version may differ from this version.

Acknowledgements:

We thank Dr. Leslie Z. Benet (UCSF) and Dr. Jasleen Sodhi (Septerna) for their critical review of the manuscript and their scientific comments and discussions.

Data Availability Statement:

The authors declare that all the data supporting the findings of this study are available within the paper and its Supplemental Data.

Authorship Contributions:

Participated in research design: Schulz Pauly, Phipps, Kalvass

Performed data analysis: Schulz Pauly, Wang

Wrote or contributed to the writing of the manuscript: Schulz Pauly, Wang, Phipps, Kalvass

DMD Fast Forward. Published on May 15, 2023 as DOI: 10.1124/dmd.123.001326
This article has not been copyedited and formatted. The final version may differ from this version.

References:

Alexandre K, and Fantin B (2018) Pharmacokinetics and Pharmacodynamics of Temocillin. *Clin Pharmacokinet* **57**:287–296.

Baker M, and Parton T (2007) Kinetic determinants of hepatic clearance: plasma protein binding and hepatic uptake. *Xenobiotica* **37**:1110–34.

Benet LZ, Liu S, and Wolfe AR (2018) The Universally Unrecognized Assumption in Predicting Drug Clearance and Organ Extraction Ratio. *Clin Pharmacol Ther* **103**:521–525.

Benet LZ, and Sodhi JK (2022) Can In Vitro–In Vivo Extrapolation Be Successful? Recognizing the Incorrect Clearance Assumptions. *Clin Pharmacol Ther* **111**:1022–1035.

Benet LZ, and Sodhi JK (2020) Investigating the Theoretical Basis for In Vitro-In Vivo Extrapolation (IVIVE) in Predicting Drug Metabolic Clearance and Proposing Future Experimental Pathways. *AAPS J* **22**:120.

Benet LZ, Sodhi JK, Makrygiorgos G, and Mesbah A (2021) There is Only One Valid Definition of Clearance: Critical Examination of Clearance Concepts Reveals the Potential for Errors in Clinical Drug Dosing Decisions. *AAPS J* **23**:67.

Bowdle TA, Patel IH, Levy RH, and Wilensky AJ (1980) Valproic acid dosage and plasma protein binding and clearance. *Clin Pharmacol Ther* **28**:486–492.

Box GEP (1976) Science and Statistics. *Journal of the American Statistical Association* **71**:791–799.

Bteich M (2019) An overview of albumin and alpha-1-acid glycoprotein main characteristics: highlighting the roles of amino acids in binding kinetics and molecular interactions. *Heliyon* **5**:e02879.

Camenisch G, and Umehara K (2012) Predicting human hepatic clearance from in vitro drug metabolism and transport data: a scientific and pharmaceutical perspective for assessing drug-drug interactions. *Biopharm Drug Dispos* **33**:179–94.

Cortellis (2022) Drug Discovery Intelligence (CDDI), Clarivate.

Diaz-Garcia JM, Evans AM, and Rowland M (1992) Application of the Axial Dispersion Model of Hepatic Drug Elimination to the Kinetics of Diazepam in the Isolated Perfused Rat Liver. *J Pharmacokinet Biop* **20**:171–193.

Fujino R, Hashizume K, Aoyama S, Maeda K, Ito K, Toshimoto K, Lee W, Ninomiya SI, and Sugiyama Y (2018) Strategies to improve the prediction accuracy of hepatic intrinsic clearance of three antidiabetic drugs: Application of the extended clearance concept and

consideration of the effect of albumin on CYP2C metabolism and OATP1B-mediated hepatic uptake. *Eur J Pharm Sci* **125**:181–192.

Hale VG, Aizawa K, Sheiner LB, and Benet LZ (1991) Disposition of prednisone and prednisolone in the perfused rabbit liver: Modeling hepatic metabolic processes. *J Pharmacokinet Biop* **19**:597–614.

Hsu SH, Cheng AC, Chang TY, Pao LH, Hsiong CH, and Wang HJ (2021) Precisely adjusting the hepatic clearance of highly extracted drugs using the modified well-stirred model. *Biomed Pharmacother* **141**:111855.

Inoue M, Hirata E, Morino Y, Nagase S, Chowdhury JR, Chowdhury NR, and Arias IM (1985) The Role of Albumin in the Hepatic Transport of Bilirubin : Studies in Mutant Analbuminemic Rats. *J Biochem* **97**:737–743.

Ito K, and Houston JB (2005) Prediction of human drug clearance from in vitro and preclinical data using physiologically based and empirical approaches. *Pharmaceut Res* **22**:103–12.

Jones DB, Morgan DJ, Mihaly GW, Webster LK, and Smallwood RA (1984) Discrimination between the venous equilibrium and sinusoidal models of hepatic drug elimination in the isolated perfused rat liver by perturbation of propranolol protein binding. *J Pharmacol Exp Ther* **229**:522–6.

Jusko WJ, and Li X (2021) Assessment of the Kochak-Benet Equation for Hepatic Clearance for the Parallel-Tube Model: Relevance of Classic Clearance Concepts in PK and PBPK. *AAPS J* **24**:5.

Kalvass JC, Phipps C, Jenkins GJ, Stuart P, Zhang X, Heinle L, Nijsen M, and Fischer V (2018) Mathematical and Experimental Validation of Flux Dialysis Method: An Improved Approach to Measure Unbound Fraction for Compounds with High Protein Binding and Other Challenging Properties. *Drug Metab Dispos* **46**:458–469.

Kochak GM (2020) Critical Analysis of Hepatic Clearance Based on an Advection Mass Transfer Model and Mass Balance. *J Pharm Sci* **109**:2059–2069.

Koch-Weser J, and Sellers EM (1976) Binding of drugs to serum albumin (first of two parts). *N Engl J Med* **294**:311–6.

Korzekwa K, and Nagar S (2023) Process and System Clearances in Pharmacokinetic Models: Our Basic Clearance Concepts are Correct. *Drug Metab Dispos* DMD-MR-2022-001060.

Krause S, and Goss KU (2018) The impact of desorption kinetics from albumin on hepatic extraction efficiency and hepatic clearance: a model study. *Arch Toxicol* **92**:2175–2182.

Li N, Badrinarayanan A, Li X, Roberts J, Hayashi M, Virk M, and Gupta A (2020) Comparison of In Vitro to In Vivo Extrapolation Approaches for Predicting Transporter-Mediated Hepatic Uptake Clearance Using Suspended Rat Hepatocytes. *Drug Metab Dispos* **48**:861–872.

Michaelis L, Menten ML, Johnson KA, and Goody RS (2011) The original Michaelis constant: translation of the 1913 Michaelis-Menten paper. *Biochemistry* **50**:8264–9.

Nation RL, Theuretzbacher U, and Tsuji BT (2018) Concentration-dependent plasma protein binding: Expect the unexpected. *Eur J Pharm Sci* **122**:341–346.

Pang KS, and Rowland M (1977a) Hepatic Clearance of Drugs. I. Theoretical Considerations of a “Well-Stirred” Model and a “Parallel Tube” Model. Influence of Hepatic Blood Flow, Plasma and Blood Cell Binding, and the Hepatocellular Enzymatic Activity on Hepatic Drug Clearance. *Journal of Pharmacokinetics and Biopharmaceutics* **5**:625–653.

Pang KS, and Rowland M (1977b) Hepatic clearance of drugs. II. Experimental evidence for acceptance of the “well-stirred” model over the “parallel tube” model using lidocaine in the perfused rat liverin situ preparation. *J Pharmacokinet Biop* **5**:655–680.

Poulin P, Kenny JR, Hop CE, and Haddad S (2012) In vitro-in vivo extrapolation of clearance: modeling hepatic metabolic clearance of highly bound drugs and comparative assessment with existing calculation methods. *J Pharm Sci* **101**:838–51.

Roberts MS, and Rowland M (1986a) A dispersion model of hepatic elimination: 1. Formulation of the model and bolus considerations. *Journal of Pharmacokinetics and Biopharmaceutics* **14**:227–260.

Roberts MS, and Rowland M (1986b) A dispersion model of hepatic elimination: 2. Steady-state considerations-influence of hepatic blood flow, binding within blood, and hepatocellular enzyme activity. *J Pharmacokinet Biop* **14**:261–288.

Rowland M, Benet LZ, and Graham GG (1973) Clearance concepts in pharmacokinetics. *J Pharmacokinet Biop* **1**:123–36.

Rowland M, Leitch D, Fleming G, and Smith B (1984) Protein Binding and Hepatic Clearance: Discrimination Between Models of Hepatic Clearance with Diazepam, a Drug of High Intrinsic Clearance, in the Isolated Perfused Rat Liver Preparation. *J Pharmacokinet Biop* **12**:129–147.

Rowland M, and Pang KS (2018) Commentary on “The Universally Unrecognized Assumption in Predicting Drug Clearance and Organ Extraction Ratio.” *Clin Pharmacol Ther* **103**:386–388.

Rowland M, and Pang KS (2022) Hepatic clearance models and IVIVE predictions. *Clin Pharmacol Ther* **111**:1205–1207.

Rowland M, Roberts MS, and Pang KS (2021) In defense of current concepts and applications of clearance in drug development and therapeutics. *Drug Metab Dispos*, doi: 10.1124/dmd.121.000637.

Schulz JA, Stresser DM, and Kalvass JC (2023) Plasma Protein-Mediated Uptake and Contradictions to the Free Drug Hypothesis: A Critical Review. *Drug Metab Rev* 1–103.

Smith SA, and Waters NJ (2018) Pharmacokinetic and Pharmacodynamic Considerations for Drugs Binding to Alpha-1-Acid Glycoprotein. *Pharm Res* **36**:30.

Sodhi JK, Wang H-J, and Benet LZ (2020) Are there any experimental perfusion data that preferentially support the dispersion and parallel tube models over the well-stirred model of organ elimination? *Drug Metab Dispos* **48**:dmd.120.090530.

Vella-Brincat JW, Begg EJ, Kirkpatrick CM, Zhang M, Chambers ST, and Gallagher K (2007) Protein binding of cefazolin is saturable in vivo both between and within patients. *Brit J Clin Pharmaco* **63**:753–7.

Wang HJ, and Benet LZ (2019) Protein Binding and Hepatic Clearance: Re-Examining the Discrimination between Models of Hepatic Clearance with Diazepam in the Isolated Perfused Rat Liver Preparation. *Drug Metab Dispos* **47**:1397–1402.

Watkins S, Madison J, Galliano M, Minchiotti L, and Putnam FW (1994) Analbuminemia: three cases resulting from different point mutations in the albumin gene. *Proc Nati Acad Sci* **91**:9417–9421.

Weisiger RA (1985) Dissociation from albumin: a potentially rate-limiting step in the clearance of substances by the liver. *Proc Natl Acad Sci U S A* **82**:1563–7.

Yadav J, Hassani ME, Sodhi J, Lauschke VM, Hartman JH, and Russell LE (2021) Recent developments in in vitro and in vivo models for improved translation of preclinical pharmacokinetics and pharmacodynamics data. *Drug Metab Rev* **53**:207–233.

Yang J, Jamei M, Yeo KR, Rostami-Hodjegan A, and Tucker GT (2007) Misuse of the Well-Stirred Model of Hepatic Drug Clearance. *Drug Metab Dispos* **35**:501–502.

Yasumori T, Nagata K, Yang SK, Chen L-S, Murayama N, Yamazoe Y, and Kato R (1993) Cytochrome P450 mediated metabolism of diazepam in human and rat: involvement of human CYP2C in N-demethylation in the substrate concentration-dependent manner. *Pharmacogenetics* **3**:291–301.

Zucker SD, Goessling W, and Gollan JL (1995) Kinetics of bilirubin transfer between serum albumin and membrane vesicles. Insight into the mechanism of organic anion delivery to the hepatocyte plasma membrane. *J Biol Chem* **270**:1074–1081.

DMD Fast Forward. Published on May 15, 2023 as DOI: 10.1124/dmd.123.001326
This article has not been copyedited and formatted. The final version may differ from this version.

Footnotes

This manuscript was sponsored and funded by AbbVie.

Conflict of Interest Statement:

All authors are employees of AbbVie and may own AbbVie stock. AbbVie contributed to the design; participated in the collection, analysis, and interpretation of data, and in writing, reviewing, and approval of the final publication. The manuscript contains no proprietary AbbVie data.

DMD Fast Forward. Published on May 15, 2023 as DOI: 10.1124/dmd.123.001326
This article has not been copyedited and formatted. The final version may differ from this version.

Figure Legends

Figure 1. Saturable albumin binding of diazepam. A) The measured unbound fraction of diazepam (1 µg/ml=3.512 µM; (Mean ± standard deviation (SD))) $f_{u,exp}$ varies with the dilution factor D of HSA compared to plasma. Non-saturable binding (solid grey line, NSB only) poorly describes the observed binding phenomena. The full saturable binding model accurately represents diazepam binding; however, non-saturable binding is negligible (black dotted line). Saturable binding with no non-saturable binding accurately represents diazepam binding (solid red line, SB only). B) The concentration dependence of $f_{u,sat}$ varies with the HSA concentration (0.025%-4%). Diazepam albumin binding is more saturable at low HSA concentrations than at high HSA concentrations (**Fig.S1**). The open circles represent the measured $f_{u,exp}$ at 3.512 µM diazepam, while the lines reflect the modeled $f_{u,sat}$ values at different HSA concentrations (0.025% - blue dashed line, 0.075% - green dashed line, 0.5% light blue dashed line, 2% - light green dashed line, 0.04% solid purple line, 0.1% - orange dotted line, 1% - light purple dotted line, 4% - solid red line).

Figure 2. Hepatic Availability and Clearance Predictions. Considering saturable plasma protein binding, the WSM (solid green line) described the hepatic availability (F(A)) and hepatic clearance (CL_H (B)) data (black circles) best, compared to PTM (red dashed line) and DM (purple dashed line). Introducing new hepatic clearance models, like the MWSM (blue dotted line), does not further improve clearance predictions when appropriate $f_{u,sat}$ values are employed (Fitting parameters in **Table2** (Mean ± SD)).

Figure 3. Hepatic Clearance Predictions. The observed $CL_{int,u}$ at different HSA concentrations were compared with the modeled $CL_{int,u}$ for the respective models. $CL_{int,u}$ for $f_{u,sat}$ (solid symbols) are more consistent across HSA concentrations than $CL_{int,u}$ for $f_{u,exp}$ (open symbols) across all four hepatic clearance models. Saturable binding improves $CL_{int,u}$ prediction accuracy across all four hepatic clearance models. Additionally, the WSM $CL_{int,u}$ (green circles) best describes the

DMD Fast Forward. Published on May 15, 2023 as DOI: 10.1124/dmd.123.001326
This article has not been copyedited and formatted. The final version may differ from this version.

observed data (Mean ± SD), while the PTM (red squares), DM (purple diamond) and MWSM (blue triangle) deviate significantly.

DMD Fast Forward. Published on May 15, 2023 as DOI: 10.1124/dmd.123.001326
This article has not been copyedited and formatted. The final version may differ from this version.

Tables

Table 1. Saturable Protein Binding Parameters.

Parameter	SB + NSB	SB only	NSB only
B_{max} [μM]	136.8	136.8	0
K_D [μM]	0.9140	0.9140	-
K_{nsb}	~$4.930*10^{-32}$	0	110
R^2 (weighted)	0.9882	0.9882	0.8601
AICc	-189.7	-193.7	-162.4

Best fit values of the saturable albumin binding parameters were derived from the IPRL datasets (Wang and Benet, 2019; Hsu *et al.*, 2021) in GraphPad Prism 9.1.0. with $1/X^2$ weighting.

DMD Fast Forward. Published on May 15, 2023 as DOI: 10.1124/dmd.123.001326
This article has not been copyedited and formatted. The final version may differ from this version.

Table 2. Unbound Intrinsic Clearance Prediction Accuracy.

	$f_{u,sat}$			
Model	**WSM**	**PTM**	**DM**	**MWSM**
Fitted $CL_{int,u}$ [ml/min]	145.4	29.03	56.27	14.43
95% Confidence Interval	131.7-157.6	24.5-31.8	50.6-61.3	12.9-14.8
R^2 (weighted)	0.9870	0.8953	0.9637	0.5463
AICc	-80.77	-51.89	-67.68	-32.16
Average Fold Deviation (AFD) Observed/Modeled	1.2±0.2	3.8±0.9	3.1±0.2	3.1±0.1
	$f_{u,exp}$			
Model	**WSM**	**PTM**	**DM**	**MWSM**
Fitted $CL_{int,u}$ [ml/min]	103.9	38.74	56.14	15.57
95% Confidence Interval	84.4-119.1.	38.4-42.2	49.2-61.8	14.3-16.0
R^2 (weighted)	0.9497	0.9275	0.9474	0.6921
AICc	-63.23	-58.42	-62.87	-37.90
Average Fold Deviation (AFD) Observed/Modeled	1.6±0.3	3.7±0.9	3.3±0.3	3.3±0.1

$CL_{int,u}$ was determined by fitting the hepatic availability (F) data for each model. Consistency of $CL_{int,u}$ across HSA concentrations was compared for the four hepatic clearance models, $f_{u,exp,}$ and $f_{u,sat}$ in GraphPad Prism 9.1.0. with 1/Y weighting. The average fold deviation (AFD) between the observed and model fitted $CL_{int,u}$ was reported as Mean ± SD.

Figure 1

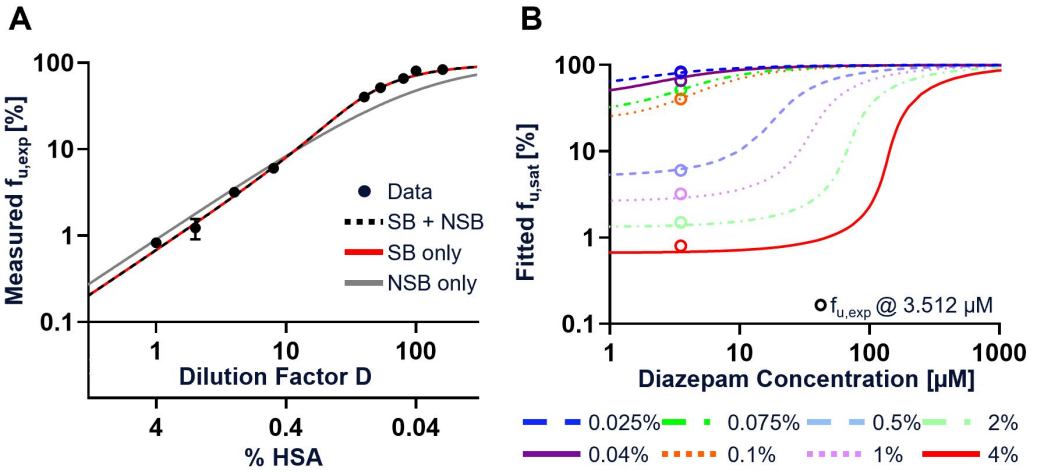
A
100
10
1
0.1
Measured $f_{u,exp}$ [%]
Data
SB + NSB
SB only
NSB only
1
10
100
Dilution Factor D
4
0.4
0.04
% HSA
B
100
10
1
0.1
Fitted $f_{u,sat}$ [%]
$f_{u,exp}$ @ 3.512 µM
1
10
100
1000
Diazepam Concentration [µM]
0.025%
0.075%
0.5%
2%
0.04%
0.1%
1%
4%

Figure 2

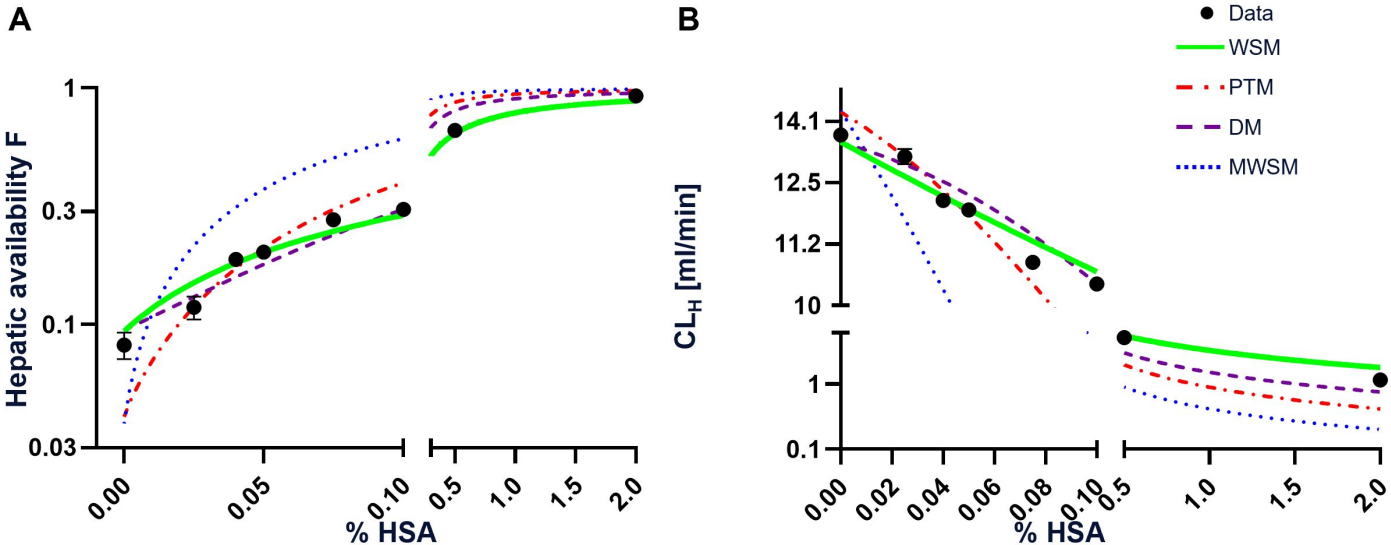
A
Hepatic availability F
1
0.3
0.1
0.03
0.00
0.05
0.10
0.5
1.0
1.5
2.0
% HSA
B
Data
WSM
PTM
DM
MWSM
CL_H [ml/min]
14.1
12.5
11.2
10
1
0.1
0.00
0.02
0.04
0.06
0.08
0.10
0.5
1.0
1.5
2.0
% HSA

Figure 3

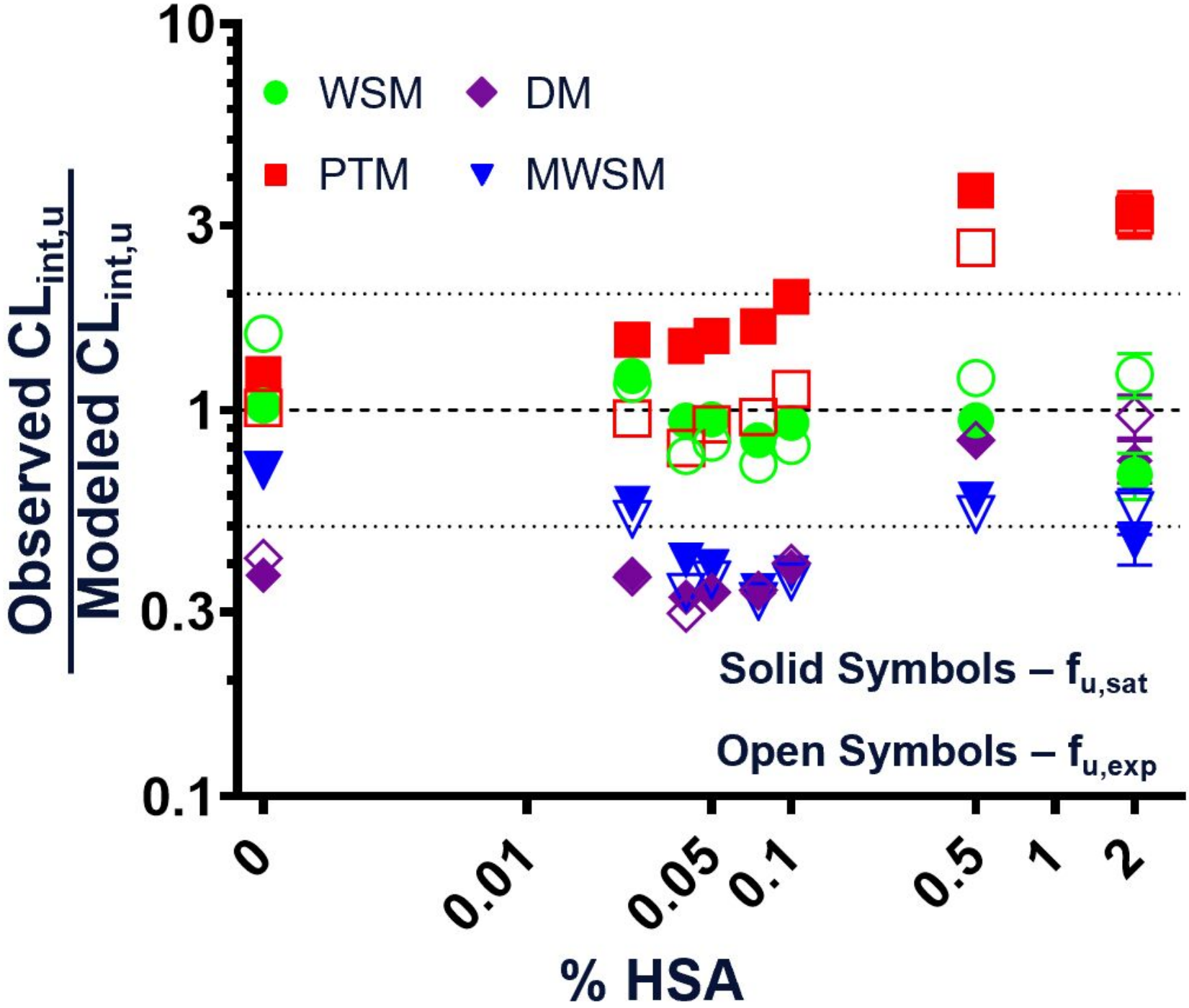
10
3
1
0.3
0.1
WSM
DM
PTM
MWSM
Observed CLint,u / Modeled CLint,u
Solid Symbols – fu,sat
Open Symbols – fu,exp
0
0.01
0.05
0.1
0.5
1
2
% HSA